Generation of micro-J pulses in the deep UV at MHz repetition rates

Research Article Vol. 4, No. 10 / October 2017 / Optica 1272

Generation of microjoule pulses in the deep ultraviolet at megahertz repetition rates

Felix Köttig,[1,*] Francesco Tani,[1] Christian Martens Biersach,[1] John C. Travers,[1,2] and Philip St.J. Russell[1]

[1]Max Planck Institute for the Science of Light, Staudtstrasse 2, 91058 Erlangen, Germany
[2]School of Engineering and Physical Sciences, Heriot-Watt University, Edinburgh EH14 4AS, UK
*Corresponding author: felix.koettig@mpl.mpg.de

Received 24 May 2017; revised 14 August 2017; accepted 22 August 2017 (Doc. ID 296672); published 12 October 2017

Although ultraviolet (UV) light is important in many areas of science and technology, there are very few if any lasers capable of delivering wavelength-tunable ultrashort UV pulses at high repetition rates. Here we report the generation of deep UV laser pulses at megahertz repetition rates and microjoule energies by means of dispersive wave (DW) emission from self-compressed solitons in gas-filled single-ring hollow-core photonic crystal fiber (SR-PCF). Pulses from an ytterbium fiber laser (~300 fs) are first compressed to <25 fs in a SR-PCF-based nonlinear compression stage and subsequently used to pump a second SR-PCF stage for broadband DW generation in the deep UV. The UV wavelength is tunable by selecting the gas species and the pressure. Through rigorous optimization of the system, in particular employing a large-core fiber filled with light noble gases, we achieve 1 μJ pulse energies in the deep UV, which is more than 10 times higher, at average powers more than four orders of magnitude greater (reaching 1 W) than previously demonstrated, with only 20 μJ pulses from the pump laser.

OCIS codes: (190.5530) Pulse propagation and temporal solitons; (190.7220) Upconversion; (060.5295) Photonic crystal fibers.

http://dx.doi.org/10.1364/OPTICA.4.001272

1. INTRODUCTION

Ultraviolet (UV) laser pulses are in great demand for a wide range of applications, including photolithography [1], spectroscopy [2], and femtosecond (fs) pump–probe measurements [3]. Despite this, the range of available sources is limited. Apart from large-scale synchrotrons and free-electron lasers, very few lasers directly emit UV light, examples being excimer and some solid-state lasers (e.g., cerium-based [4]). An alternative approach involves upconversion of visible or near-infrared laser light via the generation of discrete harmonics in $\chi^{(2)}$ and $\chi^{(3)}$ media [5,6]. Using an optical parametric amplifier as the pump laser provides wavelength-tunability in the UV, and with careful design, very short pulse durations can be achieved [7]. Although such systems are flexible, they are also complex, and repetition rate scaling is challenging because of the high pump energies required.

On the other hand, fiber and thin-disk laser technology allows repetition rate scaling in the near-infrared, pushing the frontiers of ultrafast lasers to unprecedented average power levels [8,9]. Much research is devoted to using these lasers for the generation of extreme UV light via high-harmonic generation [10,11]. To this end, pulse compression schemes are commonly employed, based, for example, on spectral broadening in bulk material [12] or gas-filled capillary and hollow-core photonic crystal fibers (HC-PCFs). This has allowed pulse compression from hundreds of fs to the few-cycle regime [13,14] and even the generation of single-cycle pulses [15].

In HC-PCFs, it is straightforward to achieve pulse compression with energies in the microjoule (μJ) to tens of μJ range based on soliton self-compression in the anomalous dispersion regime. A distinguishing feature of soliton self-compression in the presence of higher-order effects is dispersive wave (DW) emission, which is the result of phase-matching between the compressed soliton and linear waves [16,17]. Wavelength-tunable DW emission in the deep and vacuum UV has been demonstrated in gas-filled HC-PCFs [18–20], and deep UV pulses with 72 nJ energy have been generated at a 9.6 MHz repetition rate [21]. High-repetition rate (38 MHz) DW emission with 13 nJ pulse energy in the visible has also been reported [14].

Here we report the use of DW emission from self-compressed solitons in gas-filled HC-PCF to generate wavelength-tunable μJ pulses in the deep UV at close to a 2 MHz repetition rate. The pump source is a compact commercial ytterbium fiber laser (Active Fiber Systems GmbH) that delivers ~300 fs long pulses at 1030 nm with pulse energies up to tens of μJ. We show that the average power in the UV does not scale linearly with repetition rate. Through rigorous optimization of the system, in particular, employing a large-core fiber filled with light noble gases, we were able to mitigate the detrimental impact of high repetition rates on the power scaling of the DW generation. This allowed us to increase the UV pulse energy by more than 10 times (reaching 1 μJ) and the average power by more than four orders of magnitude (reaching 1 W) compared to previous results. Previous

experiments [22] and numerical simulations show that the UV pulses generated via DW emission can be as short as a few fs. The results approach schemes based on high-energy few-cycle lasers [23] but require only a fraction of the pump energy (20 μJ from a 300 fs fiber laser), are easily wavelength-tunable, and operate at orders of magnitude higher repetition rates.

2. NONLINEAR PULSE COMPRESSION

The experimental setup is sketched in Fig. 1(a). Because the pulses from the laser are too long for the direct generation of coherent UV pulses via DW emission, it was necessary to compress them in a first stage before launching them into the second stage for UV generation. In both stages, a single-ring PCF [SR-PCF—Fig. 1(d)] consisting of seven thin-walled capillaries arranged around a hollow core was used. Guiding by antiresonant reflection, SR-PCF has gained popularity because of its excellent guidance properties and simple structure. It provides broadband transmission bands with low loss (as low as 7.7 dB/km [24]), although phase-matched coupling to core-wall resonances creates high-loss bands at wavelengths $\lambda_q = [2t/(1+q)](n^2-1)^{1/2}$, where t is the capillary wall thickness, q the order of the resonance, and n is the refractive index of the glass [25]. Carefully designed fibers with small values of t provide good transmission in the near-infrared and visible spectral regions, and the impact of the loss bands on the pulse dynamics can be minimized by shifting them far from the pump wavelength. Away from these bands, the modal refractive index can be approximated by a capillary model [25], yielding anomalous dispersion in the evacuated fiber. When the fiber is filled with a noble gas, the optical Kerr effect and gas ionization are the dominant nonlinearities (the light-glass overlap is very small and the system is effectively Raman-free).

In the nonlinear compression stage, the pulses from the laser were first broadened via self-phase modulation in a noble-gas-filled SR-PCF and then compressed with negatively chirped mirrors. For our experiments, the compressor was designed to operate at an input energy of ~20 μJ. The spectral broadening was achieved in a 50 cm long SR-PCF with 53 μm core diameter and ~350 nm capillary wall thickness, filled with 23 bar Ar. The input pulses were circularly polarized, which reduces the effective Kerr nonlinearity to 2/3 of its value for linear polarization. In this way, a higher gas pressure could be used for a given input energy, resulting in weaker anomalous dispersion and higher quality compressed pulses. After the fiber, the polarization was converted back to linear. The negatively chirped mirrors (UltraFast Innovations GmbH) introduced a group delay dispersion of −2100 fs^2 to compensate for the positive chirp induced by self-phase modulation in the fiber and the dispersion of the optics up to the input of the second fiber. The pulses were measured after the nonlinear compression stage using frequency-resolved optical gating (FROG) at a 100 kHz repetition rate [Figs. 1(b) and 1(c)] or with a commercial autocorrelator at every repetition rate. The measured autocorrelation did not change significantly with repetition rate and was in good agreement with that calculated from the pulses measured via FROG at 100 kHz. At repetition rates from 100 kHz to 1.92 MHz, ~20 μJ pulses with durations of ~300 fs were compressed to <25 fs [full width at half-maximum (FWHM)] with more than 82% transmission through the compressor (including all optics). At the highest repetition rate, pulses with 20.5 μJ energy (39.3 W average power) were compressed to ~24 fs, 17.4 μJ (33.5 W) with 85% transmission. This high-efficiency pulse compression indicates that circular polarization is preserved for new spectral components generated by nonlinear processes in a gas-filled SR-PCF, over 50 cm lengths and with high peak and average powers.

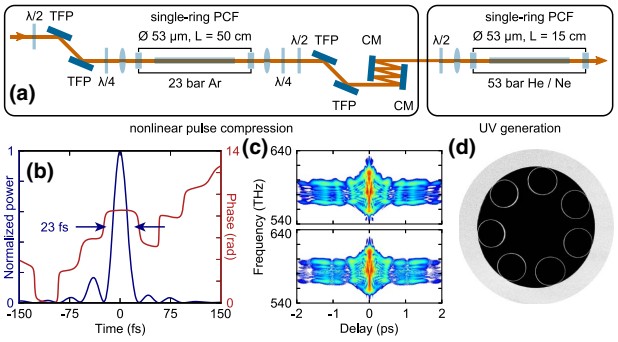

Fig. 1. (a) Experimental setup. TFP, thin-film polarizer; CM, negatively chirped mirror. (b) Temporal pulse shape at the input of the second fiber at a 100 kHz repetition rate. The pulses were measured after the nonlinear compression stage via second-harmonic generation FROG. The dispersion of subsequent optical elements was added numerically. (c) Measured (top) and retrieved (bottom) FROG trace. The colorscale covers 30 dB. (d) Scanning electron micrograph of the single-ring PCF.

3. UV GENERATION

In the second fiber stage, we used the same SR-PCF, HF-etched to reduce the capillary wall thickness to ~220 nm [the etching procedure of the SR-PCF was developed and performed by *ultralumina* (https://ultralumina.com)]. This shifted the $q = 0$ loss band from ~740 to 470 nm, reducing its impact on the pulse dynamics [26]. The fiber could in principle be etched further to allow loss-band-free transmission from the deep UV to the near-infrared. The output of the second fiber was collimated with an aluminum-coated off-axis parabolic mirror (Newport Corporation) and sent through a magnesium fluoride prism (Korth Kristalle GmbH) to spatially separate the UV. The power in the UV was then measured with a thermal power meter and corrected for the transmission of the gas cell window (5 mm thick magnesium fluoride, Thorlabs, Inc.) and the reflectivity of the parabolic mirror. The prism was cut for Brewster angle transmission at 200 nm, resulting in small Fresnel losses at the prism surfaces over the entire UV spectral region. A fiber-coupled CCD spectrometer was used to measure the spectrum.

To investigate pulse propagation in the second fiber, we performed numerical simulations based on a unidirectional field equation [27]. The nonlinearities are given by the optical Kerr effect (using the $\chi^{(3)}$ data from [28]) and photoionization (using the Perelomov *et al.* ionization rates [29]). An example is shown in Fig. 2.

The pump pulses undergo soliton dynamics when the gas pressure is adjusted for anomalous dispersion. At sufficiently high input energies, they initially compress temporally and broaden spectrally, as expected of higher-order solitons. In the experiments, the soliton order was below ~6, resulting in coherent dynamics. As the pulses compress, higher-order effects come into play. Self-steepening and the optical shock effect at the trailing edge of the pulses lead to strongly asymmetric spectral broadening toward shorter wavelengths. Phase-matching to DWs in the deep UV is made possible by higher-order dispersion and occurs when

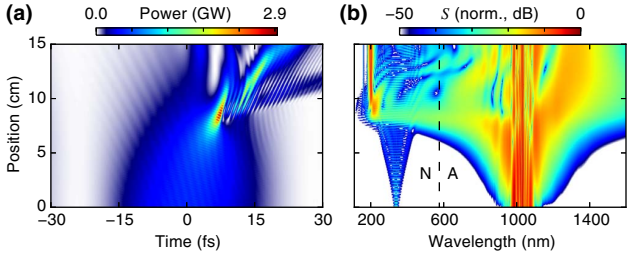

Fig. 2. Simulated (a) temporal and (b) spectral pulse propagation in a SR-PCF with 53 μm core diameter filled with 53 bar He. Input pulses as measured experimentally [Fig. 1(b)] at 17 μJ input energy. The spectral energy density S is shown per unit wavelength, normalized to its peak value. The zero-dispersion wavelength (dashed line) is at 576 nm. N and A denote regions of normal and anomalous dispersion, respectively. The input pulse self-compresses to a duration of 1.1 fs FWHM before emitting a DW at ∼200 nm, with 2 μJ energy and up to 0.3 GW peak power. The DW is emitted with a duration <10 fs and broadens to 21 fs at the fiber output (this can be avoided by optimizing the fiber length).

$\beta(\omega_{\mathrm{DW}}) = \beta_{\mathrm{sol}}(\omega_{\mathrm{DW}})$, where ω_{DW} is the DW frequency and β and β_{sol} are the propagation constants of linear waves and solitons. When this condition is not exactly satisfied, the dephasing rate takes the form $\vartheta(\omega) = \beta(\omega) - \{\beta_0 + \beta_1[\omega - \omega_{\mathrm{sol}}] + \gamma P_P \omega/\omega_{\mathrm{sol}}\}$, where β_0 is the propagation constant and β_1 is the inverse group velocity at the soliton center frequency ω_{sol}, γ is the gas-dependent nonlinear fiber parameter at ω_{sol}, and P_P is the soliton peak power. Figure 3(a) plots ϑ versus wavelength for a given set of fiber and gas parameters. The DW wavelength is widely tunable via core diameter, gas species, and pressure. Increasing the gas pressure or using a heavier gas redshifts the phase-matching point, while an increase of the peak power leads to a blueshift. Additionally, the pump pulses can undergo substantial blueshifting (through ionization) before DW emission, leading to a DW redshift. The use of lighter gases, which have higher ionization potential, typically improves conversion efficiency to the UV through reduced ionization and cleaner self-compression, as well as reduced high-repetition rate effects (this is discussed later). We therefore chose the lightest gas that allowed phase-matching at the target wavelength (up to the maximum pressure of the gas cell—60 bar).

We filled the second fiber with He and Ne to demonstrate DW emission in the deep UV at ∼200 and ∼270 nm, respectively. Figure 4(a) shows the measured spectrum after the second fiber

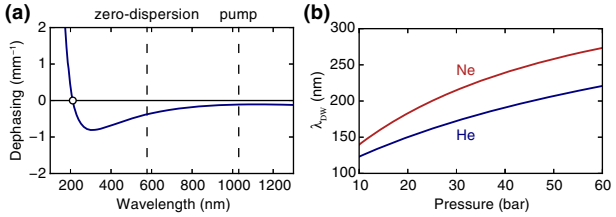

Fig. 3. Phase-matching to DWs for a fiber with 53 μm core diameter and a pump at 1030 nm with 1 GW peak power. (a) Dephasing rate ϑ for a fiber filled with 53 bar He. Phase-matching occurs at 211 nm (circle). The shallow dispersion of the gas-filled fiber yields long coherence lengths for broadband DW emission (here the coherence length exceeds 3 cm for a bandwidth of 15 nm/103 THz, corresponding to a relative bandwidth of 7.3%). (b) Phase-matching wavelength λ_{DW} as a function of pressure for He and Ne.

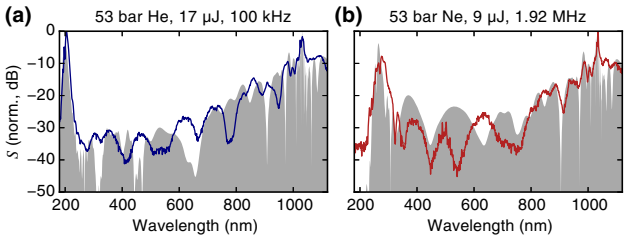

Fig. 4. (a) Measured (blue) and simulated (undershaded in gray) spectra from the second fiber when filled with He and pumped with 17 μJ pulses at a 100 kHz repetition rate. The measured pulse energy in the UV was 1.05 μJ (105 mW average power). (b) Measured (red) and simulated (gray) spectra for a fiber filled with Ne and pumped with 9 μJ pulses at 1.92 MHz. In this case, the measured pulse energy in the UV was 0.54 μJ (1.03 W average power).

when it was filled with 53 bar He and pumped with 17 μJ pulses at a 100 kHz repetition rate. The corresponding simulation (Fig. 2) is in good agreement. In this case, a DW was emitted at 205 nm with 1.05 μJ energy (6.2% of the input to the fiber), corresponding to an average power of 105 mW. The UV beam profile was in a clean fundamental mode, and the DW spectrum was broadband (7.9 nm/56 THz FWHM), supporting transform-limited pulses of 3.8 fs duration. It has previously been shown that DWs emitted from self-compressed solitons in gas-filled HC-PCFs are ultrashort (sub 5 fs in the work of Ermolov *et al.* [22]), an observation that is confirmed by the simulations presented here. For DW emission at longer wavelengths, the fiber was filled with 53 bar Ne. In this case, upon pumping with 9 μJ pulses at a 100 kHz repetition rate, a DW was emitted at 264 nm, with 0.74 μJ energy (8.2% of the input to the fiber), corresponding to an average power of 74 mW.

Having demonstrated high-energy DW emission in the deep UV, our next aim was to study how the process scales with repetition rate. Modest pump pulse energies of 10–20 μJ allow MHz repetition rates (up to 1.92 MHz in the current experiments) at only tens of watts average power. The results are summarized in Fig. 5. While the average power in the UV increased with repetition rate, the pulse energy decreased. Nevertheless, an average power of 1.03 W could be obtained at 275 nm (fiber filled with Ne, 1.92 MHz repetition rate). The corresponding spectrum is

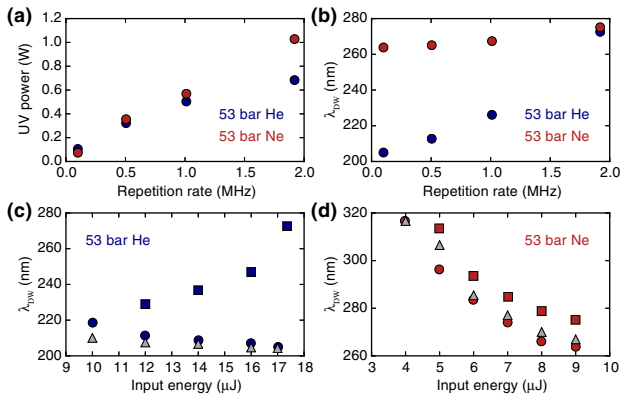

Fig. 5. (a) Power in the UV and (b) wavelength (spectral centroid) of the DWs as function of the repetition rate when the fiber was filled with He and Ne. Wavelength of the DWs as function of the input energy for the (c) He-filled and (d) Ne-filled fiber for 100 kHz (dots) and 1.92 MHz (squares) repetition rates. Gray triangles are simulated points.

shown in Fig. 4(b). In this case, the pulse energy in the UV was still 0.54 μJ, which means that 6% of the input energy to the fiber was converted to the UV.

4. DISCUSSION

As the pump energy is increased, the DW emission band typically shifts toward shorter wavelengths. This is because the self-compressed pulses have higher peak power, strengthening the Kerr contribution to the dephasing parameter ϑ. This behavior was observed for all repetition rates in the Ne-filled fiber but only at the lowest repetition rate (100 kHz) in the He-filled fiber. Instead, at 505 kHz and 1.01 MHz, the DWs initially blueshifted with increasing input energy but then redshifted as the input energy was further increased. At the highest repetition rate (1.92 MHz), the DWs continuously shifted toward longer wavelengths with increasing input energy, reaching 273 nm at the highest input energy, i.e., 68 nm/363 THz from the emission wavelength for a 100 kHz repetition rate [Fig. 5(c)]. A much smaller repetition rate dependence of the DW wavelength was observed in the Ne-filled fiber, with a redshift of only 11 nm/47 THz (264 to 275 nm) when the repetition rate was increased from 100 kHz to 1.92 MHz [Fig. 5(d)]. Although this redshift with increasing repetition rate can be partially compensated for by decreasing the gas pressure, this is at the expense of reduced conversion efficiency to the UV.

We estimate that plasma build-up over successive laser shots has a negligible impact for our experimental parameters. In any case, a constant background plasma density would make the dispersion more anomalous and lead to a blueshift of the DWs, not the observed redshift, which we attribute to small pressure-driven increases in core diameter caused by heating through nonlinear absorption and ionization (the core walls are very thin and mechanically compliant). Related high-repetition rate effects have been observed in filamentation in bulk gases [30], evolving on timescales from nanoseconds to milliseconds. While they are not yet included in established models for pulse propagation in fibers, we expect that they occur especially at high repetition rates when the system does not fully recover between successive laser shots. A difference between low (100 kHz) and high (1.92 MHz) repetition rates is more marked when the DW emission is at shorter wavelengths [Fig. 5(c)], because the strong shock effect required for efficient DW generation causes stronger ionization of the gas (according to simulations, the plasma density is up to 3.1×10^{16} cm^{-3} and the ionization-induced loss is up to 16 nJ per pulse). If, however, the DW emission is tuned to longer wavelengths [Fig. 5(d)], the required pump pulse compression is less extreme, reducing the ionization (plasma density up to 1.6×10^{15} cm^{-3} and no significant loss) and allowing better scaling with repetition rate.

To further investigate this, we filled the fiber with different gases while keeping similar dynamics—in particular, DW emission around 200 nm (Fig. 6). Already at a 100 kHz repetition rate, the UV pulse energies in Kr and Ar saturate at very low values, which is in contrast to the simulations. Only when ionization is reduced as much as possible (using Ne and He) can high pulse energies be generated in the experiments. The remaining difference could be due to fiber loss, which is neglected in the simulations, although some saturation is also visible here.

Further experiments showed an even stronger dependence on the repetition rate for fibers with smaller cores. For example, in a fiber with 36 μm core diameter, we observed lower conversion efficiency to the UV and the appearance of higher-order output modes. Since the dynamics at high repetition rates are clearly interesting for many systems operating in the strong-field regime at MHz repetition rates, we plan to investigate them further in future experiments.

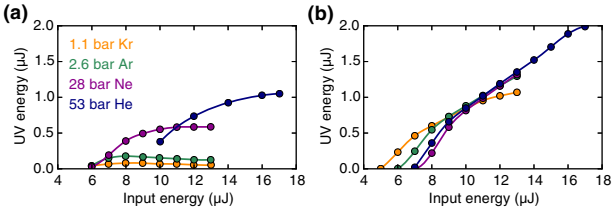

Fig. 6. UV pulse energy, (a) measured at a 100 kHz repetition rate and (b) simulated. For each gas, the pressure was adjusted so that DWs were emitted at ∼200–220 nm. In the simulations, the loss due to ionization is up to 4.7 μJ in Kr, 3.1 μJ in Ar, 0.13 μJ in Ne, and 16 nJ in He.

5. CONCLUSION AND OUTLOOK

In conclusion, high-energy deep UV pulses can be generated in gas-filled HC-PCF at repetition rates from 100 kHz to 1.92 MHz via DW emission. At 100 kHz, pulse energies of >1 μJ were obtained at 205 nm, while at 1.92 MHz, more than 1 W average power was obtained at 275 nm. Although no degradation of the SR-PCF was observed during the experiments, which lasted several hours, further studies will be required to assess the long-term stability of the system. Together with a pump laser that is carrier-envelope-phase stable, scaling to even higher repetition rates suggests the exciting possibility of bright frequency combs in the deep and maybe even the vacuum UV. Finally, the emission of DWs at short wavelengths, as demonstrated in this work, requires strong temporal self-compression of the input pulses to the single-cycle regime. Such short pulses with peak powers exceeding the GW level that can be directly delivered to a gas jet for high-harmonic generation [31] could in the near future be used to generate isolated attosecond pulses at MHz repetition rates.

REFERENCES

1. K. Jain, C. G. Willson, and B. J. Lin, "Ultrafast deep UV lithography with excimer lasers," IEEE Electron Dev. Lett. **3**, 53–55 (1982).
2. J. R. Lakowicz, *Principles of Fluorescence Spectroscopy*, 3rd ed. (Springer, 2006).
3. P. Hockett, C. Z. Bisgaard, O. J. Clarkin, and A. Stolow, "Time-resolved imaging of purely valence-electron dynamics during a chemical reaction," Nat. Phys. **7**, 612–615 (2011).
4. E. Granados, D. W. Coutts, and D. J. Spence, "Mode-locked deep ultraviolet Ce:LiCAF laser," Opt. Lett. **34**, 1660–1662 (2009).
5. J. Ringling, O. Kittelmann, F. Noack, G. Korn, and J. Squier, "Tunable femtosecond pulses in the near vacuum ultraviolet generated by frequency conversion of amplified Ti:sapphire laser pulses," Opt. Lett. **18**, 2035–2037 (1993).
6. C. G. Durfee, S. Backus, H. C. Kapteyn, and M. M. Murnane, "Intense 8-fs pulse generation in the deep ultraviolet," Opt. Lett. **24**, 697–699 (1999).
7. P. Baum, S. Lochbrunner, and E. Riedle, "Tunable sub-10-fs ultraviolet pulses generated by achromatic frequency doubling," Opt. Lett. **29**, 1686–1688 (2004).
8. M. Müller, M. Kienel, A. Klenke, T. Gottschall, E. Shestaev, M. Plötner, J. Limpert, and A. Tünnermann, "1 kW 1 mJ eight-channel ultrafast fiber laser," Opt. Lett. **41**, 3439–3442 (2016).

9. J. Brons, V. Pervak, D. Bauer, D. Sutter, O. Pronin, and F. Krausz, "Powerful 100-fs-scale Kerr-lens mode-locked thin-disk oscillator," Opt. Lett. **41**, 3567–3570 (2016).
10. S. Hädrich, A. Klenke, J. Rothhardt, M. Krebs, A. Hoffmann, O. Pronin, V. Pervak, J. Limpert, and A. Tünnermann, "High photon flux table-top coherent extreme-ultraviolet source," Nat. Photonics **8**, 779–783 (2014).
11. F. Emaury, A. Diebold, C. J. Saraceno, and U. Keller, "Compact extreme ultraviolet source at megahertz pulse repetition rate with a low-noise ultrafast thin-disk laser oscillator," Optica **2**, 980–984 (2015).
12. O. Pronin, M. Seidel, F. Lücking, J. Brons, E. Fedulova, M. Trubetskov, V. Pervak, A. Apolonski, T. Udem, and F. Krausz, "High-power multi-megahertz source of waveform-stabilized few-cycle light," Nat. Commun. **6**, 6988–6993 (2015).
13. S. Hädrich, M. Kienel, M. Müller, A. Klenke, J. Rothhardt, R. Klas, T. Gottschall, T. Eidam, A. Drozdy, P. Jójárt, Z. Várallyay, E. Cormier, K. Osvay, A. Tünnermann, and J. Limpert, "Energetic sub-2-cycle laser with 216 W average power," Opt. Lett. **41**, 4332–4335 (2016).
14. K. F. Mak, M. Seidel, O. Pronin, M. H. Frosz, A. Abdolvand, V. Pervak, A. Apolonski, F. Krausz, J. C. Travers, and P. St.J. Russell, "Compressing μJ-level pulses from 250 fs to sub-10 fs at 38-MHz repetition rate using two gas-filled hollow-core photonic crystal fiber stages," Opt. Lett. **40**, 1238–1241 (2015).
15. T. Balciunas, C. Fourcade-Dutin, G. Fan, T. Witting, A. A. Voronin, A. M. Zheltikov, F. Gerome, G. G. Paulus, A. Baltuska, and F. Benabid, "A strong-field driver in the single-cycle regime based on self-compression in a kagome fibre," Nat. Commun. **6**, 6117–6123 (2015).
16. N. Akhmediev and M. Karlsson, "Cherenkov radiation emitted by solitons in optical fibers," Phys. Rev. A **51**, 2602–2607 (1995).
17. M. Erkintalo, Y. Q. Xu, S. G. Murdoch, J. M. Dudley, and G. Genty, "Cascaded phase matching and nonlinear symmetry breaking in fiber frequency combs," Phys. Rev. Lett. **109**, 223904 (2012).
18. N. Y. Joly, J. Nold, W. Chang, P. Hölzer, A. Nazarkin, G. K. L. Wong, F. Biancalana, and P. St.J. Russell, "Bright spatially coherent wavelength-tunable deep-UV laser source using an Ar-filled photonic crystal fiber," Phys. Rev. Lett. **106**, 203901 (2011).
19. K. F. Mak, J. C. Travers, P. Hölzer, N. Y. Joly, and P. St.J. Russell, "Tunable vacuum-UV to visible ultrafast pulse source based on gas-filled Kagome-PCF," Opt. Express **21**, 10942–10953 (2013).
20. A. Ermolov, K. F. Mak, M. H. Frosz, J. C. Travers, and P. St.J. Russell, "Supercontinuum generation in the vacuum ultraviolet through dispersive-wave and soliton-plasma interaction in a noble-gas-filled hollow-core photonic crystal fiber," Phys. Rev. A **92**, 033821 (2015).
21. F. Köttig, F. Tani, P. Uebel, P. St.J. Russell, and J. C. Travers, "High average-power and energy deep-ultraviolet femtosecond pulse source driven by 10 MHz fibre-laser," in *European Conference on Lasers and Electro-Optics - European Quantum Electronics Conference* (2015), paper PD_A_7.
22. A. Ermolov, H. Valtna-Lukner, J. Travers, and P. St.J. Russell, "Characterization of few-fs deep-UV dispersive waves by ultra-broadband transient-grating XFROG," Opt. Lett. **41**, 5535–5538 (2016).
23. U. Graf, M. Fieß, M. Schultze, R. Kienberger, F. Krausz, and E. Goulielmakis, "Intense few-cycle light pulses in the deep ultraviolet," Opt. Express **16**, 18956–18963 (2008).
24. B. Debord, A. Amsanpally, M. Chafer, A. Baz, M. Maurel, J. M. Blondy, E. Hugonnot, F. Scol, L. Vincetti, F. Gérôme, and F. Benabid, "Ultralow transmission loss in inhibited-coupling guiding hollow fibers," Optica **4**, 209–217 (2017).
25. P. Uebel, M. C. Günendi, M. H. Frosz, G. Ahmed, N. N. Edavalath, J.-M. Ménard, and P. St.J. Russell, "Broadband robustly single-mode hollow-core PCF by resonant filtering of higher-order modes," Opt. Lett. **41**, 1961–1964 (2016).
26. P. Uebel, S. T. Bauerschmidt, and P. St.J. Russell, "Broadband light source device and method of creating broadband light pulses," European patent PCT/EP2017/000023.
27. F. Tani, J. C. Travers, and P. St.J. Russell, "Multimode ultrafast nonlinear optics in optical waveguides: numerical modeling and experiments in kagomé photonic-crystal fiber," J. Opt. Soc. Am. B **31**, 311–320 (2014).
28. H. J. Lehmeier, W. Leupacher, and A. Penzkofer, "Nonresonant third order hyperpolarizability of rare gases and N_2 determined by third harmonic generation," Opt. Commun. **56**, 67–72 (1985).
29. A. M. Perelomov, V. S. Popov, and M. V. Terent'ev, "Ionization of atoms in an alternating electric field," Sov. Phys. J. Exp. Theor. Phys. **23**, 924–934 (1966).
30. Y.-H. Cheng, J. K. Wahlstrand, N. Jhajj, and H. M. Milchberg, "The effect of long timescale gas dynamics on femtosecond filamentation," Opt. Express **21**, 4740–4751 (2013).
31. F. Tani, M. H. Frosz, J. C. Travers, and P. St.J. Russell, "Continuously wavelength-tunable high harmonic generation via soliton dynamics," Opt. Lett. **42**, 1768–1771 (2017).